High Resolution Fire Behavior Monitoring and Plume Simulation in the context of Experimental Fire

Ronan Paugam*[1]; William Mell[2]; Jean-Baptiste Filippi[3]; Melanie Rochoux[4], Martin Wooster[5,6]

[1]*Centre for Technological Risk Studies, Department of Chemical Engineering, Universitat Politécnica de Catalunya—BarcelonaTech, Diagonal 647, E-08028 Barcelona, Spain, {ronan.paugam@pm.me}*
[2] *Wildland Fire Science Lab, USDA Forest Service, 400 N 34th St., Suite 201, Seattle, WA 98103, USA, {william.mell@usda.gov}*
[3] *Laboratory for the Physical Systems of the Environment, Université de Corse, 20250 Corte, France, {filippi@univ-corse.fr}*
[4] *CECI, Université de Toulouse, 31100 Toulouse, France, {rochoux@cerfacs.fr}*
5 Environmental Monitoring and Modelling Research Group, Department of Geography, King's College London, London WC2R 2LS, UK
6 Leverhulme Centre for Wildfires, Environment and Society, Department of Geography, King's College London, London WC2B 4BG, UK, {martin.wooster@kcl.ac.uk}

**Corresponding author*

Keywords

Plume simulation; fire behavior; airborne observation, Experimental Fire.

Abstract

Coupled fire-atmosphere systems are currently developed to respond to the need of operational system in air quality and fire attack management. This work participates to this effort by proposing a simulation strategy where the plume is simulated using fire observation. Such approach can provide reference test case for more complex coupled fire-atmosphere simulation. Using the Forefire-MesoNH system, we simulate the plume evolution of a landscape scale burn where the fire is not simulated as a spreading front but rather prescribed from multiple fix burners controlled with observation data. The simulation of the plume formed from a 7-hectare savannah fire conducted in Kruger National Park in 2014 is demonstrated using helicopter-borne observations georeferenced at 1-m resolution and post-processed to extract information of heat fluxes at pixel level.

1. Background

Over the past 20 years, the development of earth observation (EO) satellite product enable the observation of wildfire at the global scale and show an increased of fire activity in fire-prone regions such as western USA or eastern Australia (Andela et al., 2017), most probably because of the high population living in Wildand-Urban Interface (WUI) in those regions (Doerr and Santín, 2016). To mitigate wildfire effects, operational forecast systems have been developed with either focus at fire scale for application in fire operational attack like the fire growth model FARSITE (Finney, 1998), or at plume scale for application in air quality like the Smoke Research Forecast (SRF) system BlueSky (Larkin et al., 2009).

More recently, coupled fire-atmospheres systems have been developed to resolve simultaneously the plume updraft/smoke dispersion, the propagation of the fire front, and their mutual interactions. Several coupled systems are now making references: CAWFE (Coen et al 2013), WRF-SFIRE (Mandel et al 2011) and MesoNH-ForeFire (Filippi et al 2013). While still mostly used as research tools, they are intended to become operational (Kochanski et al 2016). They are design to simulate landscape-scale (>100m) propagating fire, and therefore forced to rely on highly parameterized fire model as current computational resources cannot resolve such domain size at the resolution required to capture combustion processes that responsible of the fire front dynamics (<1cm). In atmospheric model grids, fires are set as front lines with associated Rate Of Spread (ROS)

and sensible heat flux predicted according to local orography and local modelled atmospheric variables (ie wind speed, humidity).

To the authors knowledges, apart from the recently released Rx-Cadre experiment dataset (Ottmar et al 2016), no other dataset exists that can provide simultaneous information on both the fire and the atmosphere states, and therefore can be used to run detailed validation of coupled fire-atmosphere system. Unfortunately, the prescribed burns of the Rx-Cadre experiment were set in non-homogeneous vegetation and with complex ignition pattern that make them difficult to simulate as detailed vegetation map and fast return observation of the front propagation are then required. Nevertheless, validation exercise against observation already exists for MesoNH-Forefire (Filippi et al. 2013) and WRF-SFIRE (Kochanski et al 2013). They are both based on the simulation of the Fire-Flux field work campaign which took place in 2006 (Clements et al. 2007) in a homogenous grass field in Texas. The fire was set with a single front ignition. However, no comprehensive fire behavior data were collected for this experiment, and the model validations were conducted against turbulent flux measurements acquired with an instrumented mast located along the propagation of the fire front.

2. Objective

To improve the validation of coupled fire-atmosphere system and assess further the impact of the fire model assumption on simulated fire behavior we need validation datasets for scenarios in which the fire induced winds influence fire front behavior (Liu et al 2016) as for example fire front acceleration induced by front merging. In such scenario, plume dynamics point measurement like in Clements et al. 2007 and Clements et al. 2019 are much more difficult to perform due to the more complex predictable location of best measurement point.

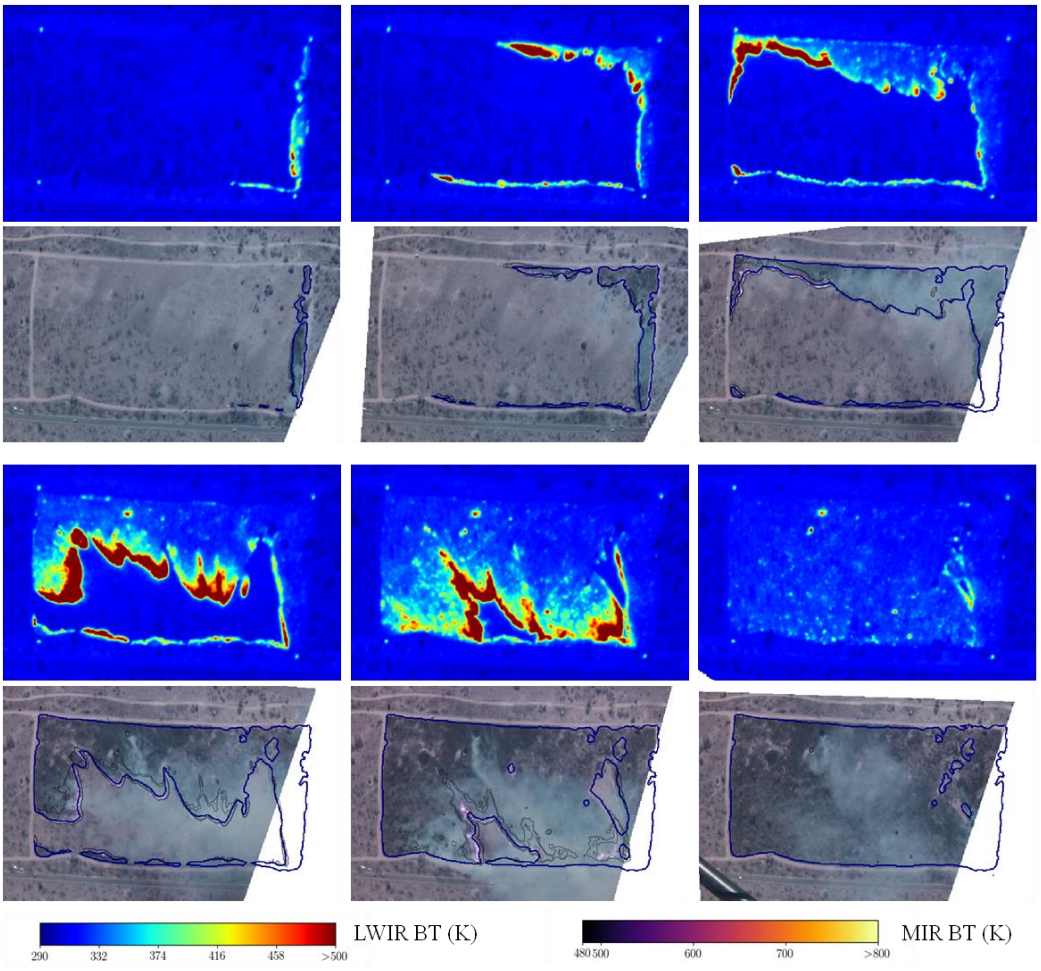

*Figure 1**: Time series of LWIR, and combined MIR/VIS images for 6 times along the 20 minutes of the duration of the Skukuza6 fire conducted on the 26th of June 2014 in Kruger National Park (South Africa). The spatial resolution is 1m for all images. Time after ignition are t=249, 419, 556, 656, 750, 931 s from top left to right bottom. Corner fires are visible on the LWIR images but were not used in the georeferencing. The VIS images show the perimeter of the active fire contour (blue line) as segmented by Convolutional Neural Network trained on the KNP dataset, and the MIR contour plot extracted from the MIR images.***

In situation of high variable fire behavior and potential complex front geometry structures, infra-red high temporal and spatial resolution observation have shown capability to capture fire front dynamics (Paugam et al 2021, Paugam et al 2022). To help continuing the development of fire-atmosphere system, we show here the potential such airborne high-resolution observation to force plume simulation.

3. High resolution experimental fire observation

We use here the orthorectified IR image data set of experimental 7-ha savannah fire processed in Paugam et al 2021. The epxeriemtal setup required to produce such data set require to have a set scene (no wildfire), but the common constraint on having bone fires presence on every image is released (Pastor et al 2012, Paugam et al 2013), hence making easier high frequency observation. The set of algorithm developed in Paugam et al 2021 are built on background feature tracking and image to image correlation optimization (Evangelidis and Psarakis 2008) for application on Long Wave Infra-Red (LWIR) and Middle Infra-Red (MIR) images. Orthorectifucation of visible image time serie are also possible if the plume is not too dense.

Results of orthorectified images collected during a fire conducted on the 26th of June 2014 on the KNP plot named Skukuza6 are shown on Fig 1. Hereafter this fire is referenced as Skukuza6. During the KNP fieldwork three cameras were operated simultaneously from a hovering helicopter:

- a visible camera (GOPRO Hero1, 1Hz, 3849x2880 pxs) with its IR filter removed to better capture flame location,
- a Long Wave Infra Red (LWIR) camera (OPTRIS 400, 7-13µm, 1Hz, 382x288 pxs, $T \in [250,1700]$
- and a Middle Infra Red (MIR) camera (FLIR AGEMA 550, 3.9 µm, 3Hz, 320x240pxs, $T \in [473,1073]$.

Fig 1 shows, for 6 times along the 20 minutes of the fire duration, LWIR images together with quasi-simultaneous combined MIR/visible images. The hovering altitude of the helicopter and the sensor resolution of the LWIR and MIR cameras allow a spatial resolution of 1m.

The second step to the image postprocessing tasks is the segmentation of the fire front. Among the 3 cameras available, we decided to base our approach on LWIR images only. This choice is explained by: (a) using only one band avoid potential problem related to time-synchronization, (b) VIS images can be masked by smoke, and (c) the MIR camera used here is not as widespread in the scientific community as the LWIR camera. The LWIR image front segmentation is based on a deep learning approach, it is described in Paugam et al 2022. Using a limited number of manually tagged front, a series of Convolutional Neural Network (CNN) is designed to develop a multiple step learning methodology gradually including information from 4 different burns. Based only on 10 initial manually segmented images, a series of 14 CNN learn front features from each other, using cumulative knowledge and manual annotation adjustment from previous front prediction. Transfer learning techniques are used to improve CNN response when including new burn to reduce overfit inherent to the first learning steps. Results of the final CNN is shown on the visible images of Fig. 1 (see blue line).

4. Plume Simulation

Using previous high-resolution fire front observation, this section intends to simulate the plume triggers by the heat flux and the emissions induced by the spreading fire front and the cooling trail located behind the front. We proposed here to use the MesoNH model (Lafore et al 1998) to simulate the atmosphere above the fire while the fire is simulated as a multitude of fix burner (one per cell of the atmospheric grid) that are switched on and off with a set strength accordingly to the fire observation (Mell and Linn 2017). The fluxes conversion from the observation resolution (1m) to the atmospheric grid (10m) is done via the ForeFire model (Filippi et al 2013). The front spread prediction of ForeFire are not used here, ForeFire control each cell as a burner where the heat flux activation is set using maps of arrival time, time of residence and total energy released. This latter is computed from the measurement of the Fire Radiative Energy (Wooster et al 2005) and an assumed radiation to total energy ratio of 10%. To better model the evolution of the fire spread each burner differentiated the phases of flaming and smoldering, so that a burner is defined with the inputs of arrival time, flaming residence time, flaming FRE, total burning time and smoldering FRE. See Fig 2 for inputs associated with the Skukuza 6 fire introduced in the previous section.

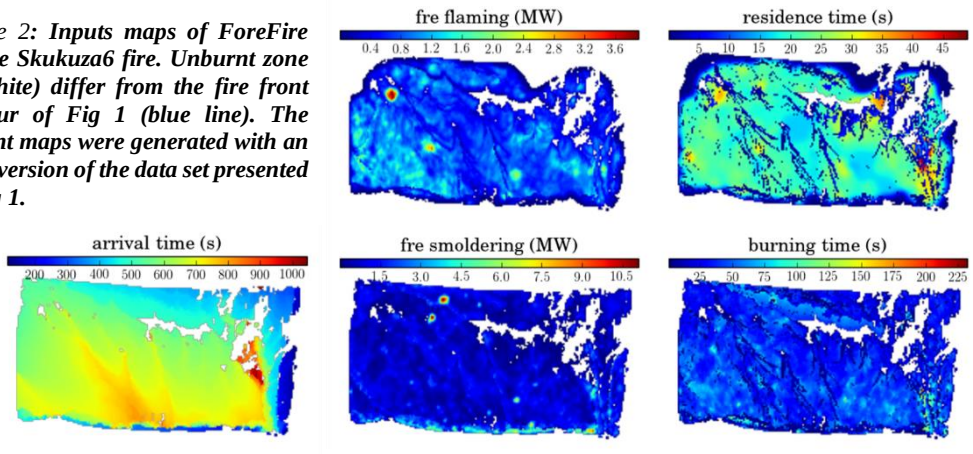

*Figure 2**: Inputs maps of ForeFire for the Skukuza6 fire. Unburnt zone (in white) differ from the fire front contour of Fig 1 (blue line). The present maps were generated with an older version of the data set presented in Fig 1.***

The arrival time map concatenates information from all the fire front CNN prediction to map the time of first appearance of the fire front in a pixel. FRE is computed from the time integration of the Fire Radiative Power that is evaluated using the MIR images following the formulation of Wooster et al 2005. The flaming residence is defined as the time is takes to a pixel ($1m^2$) to cool down below a certain threshold (here we used a MIR brightness temperature of 600K). The total burning time is the time it takes for a pixel to cool down to background temperature.

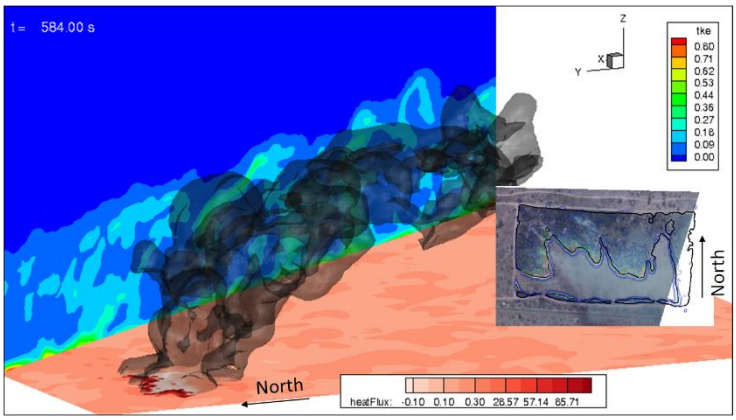

*Figure 3**: perspective view of the simulated plume of the Skukuza 6 fire a time t=584s after ignition.***

Emissions linked to the heat flux is also passed to MesoNH via the FRE formulation (Wooster et al 2005) with a conversion factor of 0.4 (kg/s/MW) and emission factors set for the flaming and the smoldering phases. In this first simulation, only a passive tracer is set. It uses emission factor of 0.05 and 0.01 for flaming and smoldering, respectively.

The MesoNH simulation uses a 10 m spatial resolution and a 4 second time step. It is run in LES mode. The initial condition is set using a radio sounding and a spin-up time of 1500 seconds that was necessary to generate the boundary layer (see tke profile on Fig 3). The radio sounding was generated from a MesoNH simulation using 3 nested models and forced with ERA interim reanalysis data. Fig 3 shows a perspective view of the plume simulated by MesoNH that was induced by fix burners set accordingly to the Skukuza 6 fire observation. The heat flux map generated by ForeFire and pass to MesoNH is seen on the ground level of the MesoNH grid.

Fig 4 shows the 10m wind data from the first level interpolated on the 2m fire data grid for 2 times of the fire evolution: at the start and end of the large ellipsoidal front spreading on the left of the plot. The fire shows a wind dominated dynamics with wind passing through the front (Finney et al 2015, Frangieh et al 2010). The wind field a ground level is significantly alter downwind to the front, see left shift southward of the front at t=600s, or the acceleration in the unburnt area at t=700s. To analyse the impact of the coupling between the fire dynamics and the wind field, Fig 5 shows correlations between the cross product of the ROS and the wind field and (a) the norm of the ROS and, and (b) the Byram's Fire Intensity (FI). FI is computed following the approach of Johnston et al (2017). In the correlation we only select point from the fire front with ROS greater than 0.2m/s to focus on the spreading part of the fronts and remove the back fire and dead front.

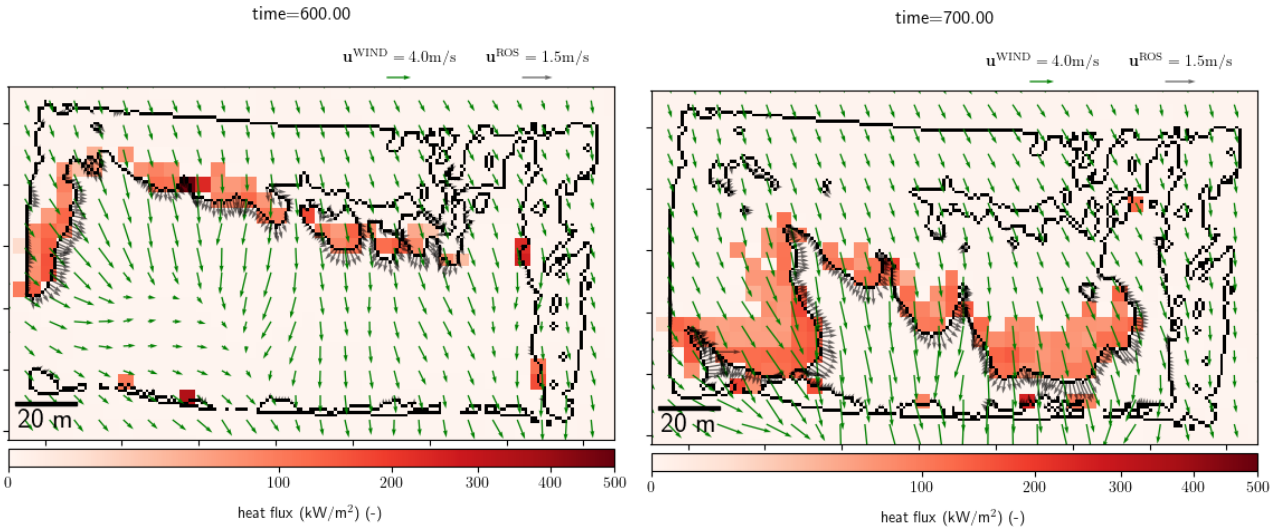

Figure 4: ***Wind vector field at 5m heigth in green (first MesoNH level) and fire front ROS in grey at 2m resolution for 2 times of the fire evolution: start and end of the main ellipsoidal front spreading on the left of the plot. The black line shows the fire front while the convective heat flux computed by the forefire flux scheme is reported in the background at the 10m MesoNH resolution.***

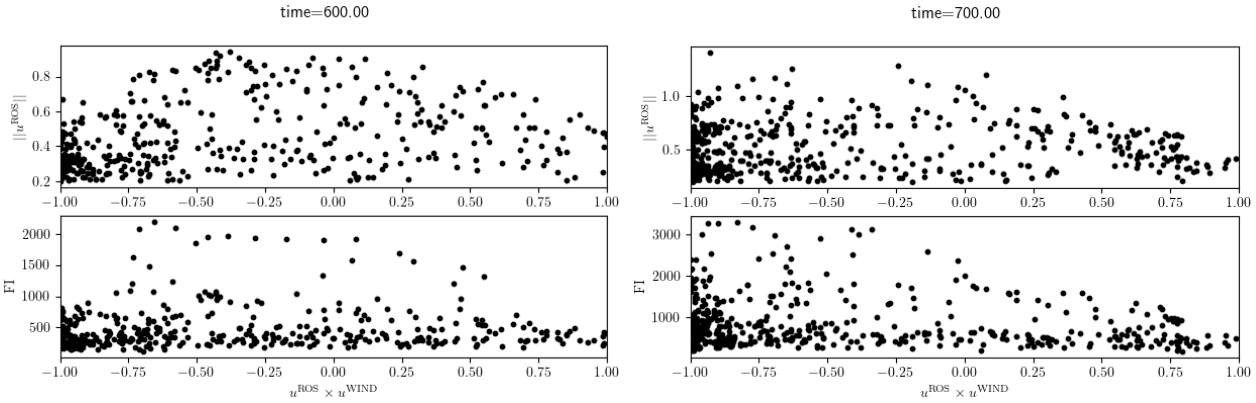

Figure 5: C***orrelation of the cross product of the ROS vector (u^{ROS}) and the wind field (u^{WIND}) with the norm of the ROS (top panels) and the Fire Intensity (FI) for the same two times t (left and right panels) as Figure 4.***

No clear correlation appears from Fig 5. The dynamics of the front does not seem to impact the wind speed near the front. This is probably due to the ambient wind direction variability that can be seen in Fig 1, for example at time t=656s, and t=750s. The ambient wind oscilates between west and south during the fire evolution as shown by smoke released by smodlering spots in the back of the fire. This variability is not taken into account in the MesoNH simulation that uses a single radio sounding and a spin-up time to build its boundary layer. As a result the ellipsoidal front spreading from the left of the plot edge is spreading in the MesoNH simulation with a southwards wind (see Fig 4 left panel) when visible image shows a clear eastwards wind at this time. This issue shows also with a right shift of the the wind field from the ROS direction in Fig5, see the large number of negative cross product at t=700s. Improving the ambient wind input will be investigated in future work as well as the impact of the heat release scheme use in forefire. Comparison with the default nominal flux of Filippi et al (2013) will be considered.

5. Conclusion and Perspectives

This work presents the development of a methodology to simulate fire plume from airborne IR observation. Unfortunately, as no atmospheric data or plume sampling were collected during the burn we simulate, no validation of the simulated plume can be run. Furthermore, no details fuel load was performed, hence making fully coupled fire-atmosphere simulation more challenging. This first attempt to simulate a plume from fire

observation is therefore only a proof of concept that emphasize use of airborne IR observation in the on-going effort of the fire community in developing fire-atmosphere coupled models. Details knowledge of plume structure and composition also shows potential application in current effort in 3D radiative transfer simulation in fire scene (Paugam et al 2021b).

Acknowledgment:
This work has received funding from the European Union's Horizon 2020 research and innovation program under the Marie Skłodowska-Curie, grant H2020-MSCA-IF-2019-892463.

References:

Andela, N.,et al: A human-driven decline in global burned area, Science, 356, 1356–1362, doi:10.1126/science.aal4108, 2017.
Clements C. B., S. et al: FireFlux A Field Validation Experiment, Bulletin of the Am. Met. Soc. 88 (2007) 1369–1382.
Clements Craig B., et al (2019) The FireFlux II experiment: a model-guided field experiment to improve understanding of fire–atmosphere interactions and fire spread. International Journal of Wildland Fire 28, 308-326.
Coen, J.L. Modeling Wildland Fires: Of the Coupled Atmosphere-Wildland Fire Environment Model (CAWFE); Technical Report, NCAR Technical Note NCAR/TN-500+STR; NCAR: Boulder, CO, USA, 2013.
Doerr SH, Santı´n C. 2016 Global trends in wildfire and its impacts: perceptions versus realities in a changing world. Phil. Trans. R. Soc. B 371: 20150345. http://dx.doi.org/10.1098/rstb.2015.0345
Evangelidis G , Psarakis E . Parametric Image Alignment Using Enhanced CorrelationCoefficient Maximization. IEEE Transactions on Pattern Analysis and Machine Intelligence, Instituteof Electrical and Electronics Engineers, 2008, 30 (10), pp.1858-1865.
Filippi J.-B., et al, Assessment of ForeFire/Meso-NH for wildland fire/atmosphere coupled simulation of the FireFlux experiment, Proceedings of the Combustion Institute 34 (2013) 2633–2640.
Finney, M. A.: FARSITE: Fire Area Simulator-model development and evaluation, Tech. rep., U.S. Department of Agriculture, Forest Service, Rocky Mountain Research Station, Ogden, doi:10.2737/RMRS-RP-4, 1998.
Finney et al, Role of buoyant flame dynamics in wildfire spread, 112 (32) 9833-9838, PNAS, 2015
Frangieh, Accary, Morvan, Méradji, Bessonov, Wildfires front dynamics: 3D structures and intensity at small and large scales, Combustion and Flame, Volume 211, 2020, Pages 54-67,
Johnston, Joshua, Wooster, Martin, Paugam, Ronan, Wang, Xianli, Lynham, Timothy, Johnston, Lynn. (2017). Direct estimation of Byram's fire intensity from infrared remote sensing imagery. International Journal of Wildland Fire. 26. 668-684. 10.1071/WF16178.
Kochanski A. et al, Evaluation of WRF-SFIRE performance with field observations from the FireFlux experiment, Geoscientific Model Development 6 (2013) 1109–1126.
Kochanski A. et al, Toward an integrated system for fire, smoke and air quality simulations, IJW F25 (2016) 534.
Lafore, J. P., et al. The Meso-NH Atmospheric Simulation System. Part I: adiabatic formulation and control simulations, Ann. Geophys., 16, 90–109, 1998.
Larkin, N. K., et al : The BlueSky smoke modeling framework, International Journal of Wildland Fire, 18, 906, doi:10.1071/WF07086, 2009.
Liu Yongqiang, et al. 2017. Fire and Smoke Model Evaluation Experiment (FASMEE): Modeling gaps and data needs. In: Proceedings for the 2nd International Smoke Symposium November; 14-17, 2016, Long Beach, California, USA. Missoula, MT: International Association of Wildland Fire. 13 p.
Mandel, J.; et al.: Coupled atmosphere-wildland fire modeling with WRF 3.3 and SFIRE. Geosci. Model Dev. 2011, 4, 591–610.
Mell, W.E.; Linn, R.R. FIRETEC and WFDS Modeling of Fire Behavior and Smoke in Support of FASMEE—Final Report to the Joint Fire Science Program | FRAMES. 2017.
Ottmar R. D., J. K. Hiers, B. W. Butler, C. B. Clements, M. B. Dickinson, A. T. Hudak, J. J. O'Brien, B. E. Potter, E. M. Rowell, T. M. Strand, T. J. Zajkowski, Measurements, datasets and preliminary results from the RxCADRE project 2008, 2011 and 2012, IJWF 25 (2016) 1.
Pastor E., E. Planas, Infrared imagery on wildfire research. Some examples of sound capabilities and applications, in: 2012 3rd International Conference on Image Processing Theory, Tools and Applications, IPTA 2012, IEEE, 2012, pp. 31–36.
Paugam R., et al, Use of handheld thermal imager data for airborne mapping of fire radiative power and energy and flame front rate of spread, IEEE Transactions on Geoscience and Remote Sensing 51 (2013) 3385–3399.
Paugam, et al 2021b. 3DFireLab: a Virtual Fire Scene Simulator for the Simulation of Infra Red Fire Observation. 13th IAFSS Symposium, Waterloo CA, 26-30 April 2021.
Paugam, R. et al Orthorectification of Helicopter-Borne High Resolution Experimental Burn Observation from Infra Red Handheld Imagers. Remote Sens. 2021, 13
Paugam, R. et al Fire front segmentation and rate of spread estimation from airborne thermal infra red observation using deep learning, Int. J. Wildland Fire, 2022, (submitted in Mars 2022)
Wooster M.et al. Retrieval of biomass combustion rates and totals from fire radiative power observations: FRP derivation and calibration relationships between biomass consumption and fire radiative energy release, Journal of Geophysical Research Atmospheres 110 (2005) 1–24.